

Biogeosciences Discussions is the access reviewed discussion forum of *Biogeosciences*

Oxygen penetration deep into the sediment of the South Pacific gyre

J. P. Fischer¹, T. G. Ferdelman¹, S. D'Hondt², H. Røy³, and F. Wenzhöfer¹

¹Max Planck Institute for Marine Microbiology, Bremen, Germany

²Graduate School of Oceanography, University of Rhode Island, USA

³Center for Geomicrobiology, University of Aarhus, Denmark

Received: 3 March 2009 – Accepted: 13 March 2009 – Published: 19 March 2009

Correspondence to: J. P. Fischer (jfischer@mpi-bremen.de)

Published by Copernicus Publications on behalf of the European Geosciences Union.

3159

Abstract

Benthic microbial oxygen consumption rates were investigated during an IODP site survey to the South Pacific Gyre. Primary production, particle fluxes and sedimentation rates are extraordinarily low in this most oligotrophic oceanic region on earth. We studied benthic microbial respiration rates from vertical oxygen profiles in sediments obtained on different spatial scales *ex situ* (in piston cores and multi cores), and *in situ* (using a benthic lander with a microelectrode profiler). Along a transect in the area 24 to 46° S and 165 to 117° W, cores at 10 of 11 sites were oxygenated for their entire lengths (as much as 8 m below seafloor), at concentrations $>150 \mu\text{mol L}^{-1} \text{O}_2$. This represents the deepest oxygen penetration ever measured in marine sediments. Microprofiles from the top sediment layer revealed a diffusive oxygen flux to the sediment in the order of $0.2 \text{ mmol m}^{-2} \text{ d}^{-1}$. This is in the lower range of previously reported fluxes for oligotrophic sediments but corresponds well to the low surface water primary production. Because of the inert nature of the deeper sediment, oxygen that is not consumed in the surface layer diffuses downward to much greater depth. In deeper zones, a small O_2 flux of $\sim 0.1 \mu\text{mol m}^{-2} \text{ d}^{-1}$ was therefore still present. This flux was constant with depth, indicating extremely low respiration rates. Modeling of the measured oxygen profiles suggests that the sediment is probably oxygenated down to the basalt, indicating an oxygen flux from the sediment into the basaltic basement.

1 Introduction

Interpretation of oxygen profiles is a common way to assess benthic microbial processes since the relation between oxic respiration and remineralization rates in sediments is nearly quantitative (Thamdrup and Canfield, 2000; Bender and Heggie, 1984). Oxygen concentration profiles thus contain information about the magnitude and vertical organization of carbon turnover. The depth of the oxic-anoxic interface is regulated by the balance between oxygen consumption (respiration and re-oxidation of the

3160

reduced products from anaerobic metabolism) and oxygen transport (diffusion, advection, bio-irrigation). Due to the low flux of particulate organic matter in deep ocean gyres, only low rates of carbon mineralization can be sustained and therefore, deep oxygen penetration can be expected. Wenzhöfer et al. (2001) found an oxygen penetration depth of ~ 25 cm in the central South Atlantic and earlier studies in the central Pacific found oxygen concentrations decreasing with depth only in the top layer and showing very little if any change with depth below 20–40 cm (Murray and Grundmanis, 1980).

The South Pacific gyre (SPG) is the largest oligotrophic marine environment on earth (Claustre and Maritorena, 2003). It is farther away from continents than any other oceanic region and hence it has very little aeolian and fluvial input. The surface water of the SPG is characterized by chlorophyll concentrations below 20 g m^{-3} (Ras et al., 2008) and these waters are among the clearest on earth in terms of UV absorption (Morel et al., 2007). The low surface water productivity results in low sedimentation rates which vary between 0.08 and 1.1 mm kyr^{-1} (D'Hondt et al., 2009). In general, sediments of the SPG have received little scientific interest since the 1901 expedition of the S.S. *Brittania* described them as oceanic red-clays with manganese nodules. The whole area is largely understudied compared to other oceanic regions (Daneri and Quinones, 2001) and little is known about the carbon cycle in the seabed. Since the overall area of oligotrophic subtropical gyres represent up to 60% of the global oceans (Claustre et al., 2008), their importance for the system earth is evident. A recent study by D'Hondt et al. (2009) provides evidence that these sediments harbor subseafloor communities with microbial cell abundances several orders of magnitude lower than in all previously described subseafloor environments with extremely low aerobic metabolic activities throughout the entire core (D'Hondt et al., 2009). While said study mainly focusses on the deep subseafloor and presents an overview of the results of the whole cruise, we further investigated the deep oxygen profiles, combined them with micro-profiles of the top sediment layer and explored the implications of these data in terms of depth-resolved fluxes and respiration rates by mathematical modeling.

3161

To investigate the oxygen flux in oligotrophic sediments, in situ and ex situ measurements with microsensors were performed using a free-falling benthic lander (Reimers et al., 1986; Wenzhöfer and Glud, 2002) and a multi-coring device, respectively. The high resolution profiles obtained from the uppermost active first centimeters were used to calculate the diffusive oxygen flux into the sediment. Additionally, a special set-up for onboard measurements of oxygen concentrations in long piston and gravity cores was developed. Combining these methods allowed us to gain a comprehensive picture of the respiration rates in the first decimeters of the sediment down to several metres. Extrapolating the profiles down to the basalt and the application of reaction-diffusion models gave further insight into respiration rates in deeper layers. The benthic mineralization capacity of the ultra-oligotrophic sediments of the South Pacific is discussed in comparison to other oligotrophic environments.

2 Material and methods

2.1 Study site

During the KNOX-02RRR expedition (17 December 2006–27 January 2007), we sampled sediment cores at 11 stations within the region 24° S to 46° S and 165° W to 117° W (Fig. 1). The cruise track can be divided into two transects: one northern transect at a latitude of 24° S to 27° S , ranging from older crust ($\sim 100 \text{ Ma}$) to younger ($\sim 6 \text{ Ma}$) and at the same time from the outer portion of the gyre to its center. The southern transect at latitude of 38° S to 45° S leads out of the gyre toward older crust ($\sim 75 \text{ Ma}$) (Fig. 1). To get a comprehensive picture of oxygen profiles in low-activity sediments, different methods were used for their investigation at different spatial scales. Oxygen profiles in the top few centimeters of the sediments were measured with microelectrode profiling top down, both in situ with a benthic lander and ex situ in recovered cores. To investigate deeper sediment layers, oxygen concentrations were measured ex situ with needle-shaped optical sensors through drilled holes in the piston core liner.

3162

2.2 In situ measurements

A free falling, programmable benthic lander was used to measure oxygen profiles in the top centimeters in situ with high resolution (Wenzhöfer and Glud, 2002; Archer et al., 1989). The lander was equipped with a microelectrode profiler enabling profiling in 100 μm steps, down to 5 cm. On-board sensor calibration prior to the deployment was performed with air-saturated and anoxic seawater at in situ temperature. The obtained profiles were used to calculate diffusive fluxes into the sediment, using Fick's first law of diffusion (Berner, 1980). Since the diffusive boundary layer (DBL) could not accurately be determined from the profiles, the flux was calculated from gradients just below the sediment surface, using a sediment diffusion coefficient of $6.7 \times 10^{-6} \text{ cm}^2 \text{ s}^{-1}$ as determined from the average formation factor of the sediment (see below).

2.3 Ex situ measurements on multi-cores

To study the top sediment layer in more detail, sediment was recovered using a Multiple Corer (Barnett et al., 1984). These cores appeared undisturbed with intact microstructure at the sediment surface. Immediately after recovery, the sealed tubes were stored at 4°C. Small rotating magnets ensured well-mixed overlying waters and a DBL thickness close to the in situ conditions (Rasmussen, 1992; Glud et al., 1994). Oxygen profiles were measured on 5 of the 11 stations with Clark-Type microelectrodes (Revsbech, 1989), a custom-made picoamperemeter, an A/D converter (DAQPad-6020E, National Instruments) and a motorized stage (VT-80, Micos GmbH, Germany). In some cores, the oxygen concentration in the overlying water was changed by air bubbling and transient profiles were recorded over 24 h. Raising the bottom water oxygen concentration in a multi-core from $280 \mu\text{mol L}^{-1}$ to $310 \mu\text{mol L}^{-1}$ caused an oxygen front to diffuse into the sediment (Fig. 2). Using the Einstein-Smoluchowski Equation (e.g. Revsbech and Jørgensen, 1983), the speed of this front was used to calculate the effective diffusion coefficient as $6 \times 10^{-6} \text{ cm}^2 \text{ s}^{-1}$. The good agreement with the value obtained using the average formation factor (Sect. 2.5) highlights the inert nature of the sediment.

3163

2.4 Ex situ measurements on piston cores

We compared measurements with clark-type microelectrodes and needle optodes on both, piston cores and trigger cores (which operate like gravity cores) of Station 1 and 2 and found no significant difference in oxygen profiles (data not shown). However, the signals of the optodes were found to be more stable and accurate. Since optodes are also mechanically more robust, they were used for all later measurements. The optode itself consisted of a fiber optic cable (125 μm \emptyset), glued into a stainless steel capillary which itself was reinforced by another stainless steel tube into which the capillary was fit (Klimant et al., 1995; Wenzhöfer et al., 2001). The fiber tip was polished using lapping film with decreasing grain size, down to 0.5 μm (3M Inc.). The sensing dye consisted of 2% platinum(II) mesotetra (pentafluorophenyl) porphyrin (Frontier Scientific, Inc.) in a polystyrene matrix. To coat the fiber tip, the mixture was dissolved in chloroform and applied under a microscope using a micromanipulator. Optode readout was done using a MICROX TX3 (PreSens Precision Sensing GmbH) optode meter. A two-point calibration was done using anoxic and air-saturated seawater at room temperature about every 2 h. Conversion of the measured fluorescence lifetime of the optode to oxygen values using a modified Stern-Vollmer equation was done internally by the instrument.

After recovery, the piston cores were cut into sections of 150 cm and the ends were sealed with PVC caps and adhesive tape. The cores were allowed to thermally equilibrate for at least 24 h in the lab at 20°C before the measurements started. Immediately prior to each measurement, two 6 mm \emptyset holes were drilled through the core liner in close vicinity to each other using a spiral drill with a stop unit to prevent drill penetration into the sediment. The self-made fiber optode was inserted through one of the holes into the center of the core and a temperature probe for thermal compensation was inserted through the second hole. For the first 50 cm of the piston core, measurements were done in 10-cm intervals, while the remaining core was measured in 20–30 cm intervals. After insertion of the optode into the center of the core, the sensor was allowed

3164

to equilibrate for about 15 min, before the optode readout was averaged over 5 min. A randomized order of measurements along the core prevented measurement drift artifacts. To ensure that the center of the core was unaffected by ambient air that diffused into the core after recovery, radial microsensor profiles with a Clark-type microsensor were done on a core that was sitting in the lab for 32 h. In a distance of about 2 cm from the core liner, the oxygen profile leveled off, as expected by model calculations, revealing that the center of the 10 cm Ø core was undisturbed (data not shown).

2.5 Modeling

Our analysis of the measured oxygen profiles included mathematical modeling of transient and steady-state mass balance of oxygen in the pore water. We used different models to analyze the different aspects of the data. To extrapolate the deep profiles down to the basalt (Fig. 3), we fitted an exponential function to the measured data points:

$$c(\text{O}_2)(z) = \alpha e^{-\beta z} \quad (1)$$

where z is the depth and α and β are fit parameters. Since it is likely that the first meter of the piston core was disturbed during coring (Buckley et al., 1994; Skinner and McCave, 2003), we excluded these data points from the fit. This simple model implies a single, exponentially decreasing respiration rate as well as flux of oxygen with depth. For further analysis including fluxes to the basalt and intercomparison of the deep profiles, a one-dimensional reaction-diffusion model was set up. We assumed steady state conditions and a fixed bottom water concentration as measured. The formation factor F , the ratio of the electric resistivity of the bulk sediment to the resistivity of the unrestricted porewater, was used to calculate the sediment's diffusion coefficient (Berner, 1980). It was virtually constant with depth and between the different sites (KNOX-02RR expedition report, 2007). Therefore, we choose a constant effective diffusion coefficient for all calculations: $D_0/F = D_s \phi = 6.7 \times 10^{-10} \text{ m}^2 \text{ s}^{-1}$. The diffusion coefficient of oxygen in free solution (D_0) was taken from Schulz and Zabel (2000) and corrected for in situ

3165

salinity and temperature (Li and Gregory, 1974). Since bioturbation and sedimentation rates can be neglected in the SPG, the 1-D-model can be formulated as:

$$\frac{D_o}{F} \frac{\partial^2 c(\text{O}_2)}{\partial z^2} - \left(\frac{\partial c(\text{O}_2)}{\partial t} \right)_{\text{res}} = 0 \quad (2)$$

Where z is the depth and $c(\text{O}_2)$ is the oxygen concentration at depth z . In this model, the respiration rate was constant with depth and we assumed a constant flux of oxygen at the sediment/basalt interface (z_{max}) for each site:

$$J = - \frac{D_o}{F} \frac{\partial c(\text{O}_2)}{\partial z_{\text{max}}} = \text{const.} \quad (3)$$

To test for plausible combinations of flux to the basalt and respiration rate, both parameters were varied simultaneously in a parameter variation study and the resulting modeled profiles were compared to the measured profiles, calculating r^2 values for the goodness of fit. To avoid negative concentrations, a Michaelis-Menten type kinetics of the respiring community was assumed with a small K_m value of $0.1 \mu\text{mol L}^{-1}$:

$$\frac{\partial c(\text{O}_2)}{\partial t} = \text{resp}_{\text{max}} \frac{c(\text{O}_2)}{K_m + c(\text{O}_2)} \quad (4)$$

where resp_{max} represents the varied respiration rate. The oxygen concentrations that drive the mass balance are mostly far above K_m . Therefore, the exact value of K_m is not important and the rates expressed in the model are generally close to resp_{max} if oxygen is present. The model was implemented using the finite element modeling software COMSOL (COMSOL AB, Stockholm). Post-processing was done with Matlab scripts (MathWorks, Inc.). To include the surface ($z < 5 \text{ cm}$) of the sediment column, a separate model was used to account for the much higher gradients in this sediment layer. Here, an exponentially decreasing respiration rate with depth was assumed to represent the top layer with a constant offset for the deep respiration. The respiration

term in Eq. (2) for this model reads therefore:

$$\frac{\partial c(\text{O}_2)}{\partial t} = \text{resp}_{\text{max}} e^{-\alpha z} + \text{resp}_{\text{const}} \quad (5)$$

The effects of the constant respiration rate $\text{resp}_{\text{const}}$ and the exponential decay factor α were studied by parameter variation. The goodness of the resulting modeled profiles was again assessed by calculating r^2 values for the comparison with measured microsensor profiles.

2.6 Calculation of carbon input

Several empirical models have been proposed for the calculation of the carbon flux to oceanic sediments from primary production in surface waters (e.g. Berger et al., 1987; Betzer et al., 1984; Pace et al., 1987; Suess, 1980). Specific models for oligotrophic regions, however, do not exist. The model composed by Antia et al. (2001) was used in this study ($J_{\text{POC}_A} = 0.1 P P^{1.77} Z^{-0.68}$) since it represents an average of the cited models. Primary production values were taken from SeaWiFs remote sensing data, converted into integrated annual primary productivity by the IMCS Ocean Primary Productivity Team (Rutgers, State University of New Jersey) using the algorithms from Behrenfeld and Falkowski (1997).

To convert the measured oxygen fluxes into fluxes of labile organic carbon (J_{POC_R}) necessary to sustain these rates, we used the Redfield-Ratio (C:O=106:138) as an approximation.

20 3 Results and discussion

The major biogeochemical processes in sediments can be divided into transport phenomena and reaction processes. In general, important vertical transport processes in marine sediments are bioturbation/bioirrigation, advection and molecular diffusion (Berg et al., 2001). Since we found no traces of zoobenthos in the SPG, bioturbation

3167

and bioirrigation are likely to be irrelevant; the low permeability of the clay sediments also excludes any appreciable advection. Therefore, molecular diffusion is the only relevant transport process in these oligotrophic sediments and, together with biogeochemical reactions (e.g. respiration and reoxidation), controls the penetration of oxygen into the sediment.

3.1 Benthic carbon fluxes

Microsensor oxygen profiles of the uppermost sediment layer were measured ex situ in recovered sediment cores (Stations 4–7) and in situ (Station 10) (Fig. 4). A general trend of decreasing oxygen fluxes toward the center of the gyre was observed (Table 1), varying between $0.13 \text{ mmol m}^{-2} \text{ d}^{-1}$ (Station 7, the middle of the gyre) and $0.32 \text{ mmol m}^{-2} \text{ d}^{-1}$ (Station 10, close to the edge of the gyre). It is however known that ex situ measurements of oxygen profiles are biased by core recovery artifacts, tending to underestimate the oxygen penetration depth and to overestimate the calculated benthic flux (e.g. Glud et al., 1994). Sediment decompression and warming as well as enhanced availability of labile organic matter are considered as possible explanations. These findings result from investigations in highly productive areas with high gradients and low oxygen penetration depth. Since our measurements were performed in low-productivity regions with deep oxygen penetration and low microbial activities, only little differences between in situ and ex situ results are to be expected.

The measured oxygen fluxes are slightly lower compared to previously reported fluxes from oligotrophic sediments in the Atlantic ($>0.3 \text{ mmol m}^{-2} \text{ d}^{-1}$ (Wenzhöfer and Glud, 2002; Wenzhöfer et al., 2001), but at the upper end of fluxes measured in the central equatorial Pacific ($0.013\text{--}0.22 \text{ mmol m}^{-2} \text{ d}^{-1}$), even though there is a lower primary production in the surface-water of the SPG. However, the coarse sampling resolution of several centimeters by Murray and Grundmanis (1980) very likely underestimates the oxygen consumption at the sediment-water interface.

Since the vast majority of the rain of organic matter that reach the seafloor is ultimately oxidized, oxygen fluxes can be used to calculate organic particle fluxes (Jahnke,

3168

1996). Converting our measured oxygen fluxes into carbon equivalents, assuming a stoichiometry of C:O=106:138 resulted in carbon fluxes (J_{POC_R}) between 0.45 and 1.06 $\text{gC m}^{-2} \text{yr}^{-1}$, with a mean of 0.72 $\text{gC m}^{-2} \text{yr}^{-1}$ (Table 1). These carbon fluxes are in the same order of magnitude as fluxes reported for the deep North Pacific (Murray and Kuivila, 1990) and they agree well with the extrapolations of Jahnke (1996) for the SPG. The decrease of fluxes towards the center of the gyre is reflected by the lower surface water primary production, indicating that the benthic mineralization is primarily fueled by the export of organic matter from surface waters. Using remote sensing data of PP (Behrenfeld and Falkowski, 1997) and an empirical model for carbon export to deep waters (Antia et al., 2001) permits estimation of particulate organic carbon (J_{POC_A}) fluxes to the sediment. However, these fluxes calculated from PP data exceed the fluxes derived from oxygen profiles (J_{POC_R}) by 14% (Station 5) to 54% (Station 7). The only exception is Station 4, where J_{POC_R} is 26% higher than J_{POC_A} . Differences between J_{POC_R} and J_{POC_A} were not correlated to surface chlorophyll concentrations or sedimentation rates. One cause for the differences may be the assumption of constant porosity in the surface layer that might lead to slight underestimation of surface oxygen fluxes. This effect could possibly raise the J_{POC_R} up by 15%, if the surface porosity was 0.9 (Barrer, 1946). Another more likely explanation for the discrepancy may be that the empirical algorithms used to correlate chlorophyll a content to ocean color are based mostly on data points in the Northern Hemisphere with few points from oligotrophic gyres (Claustre and Maritorena, 2003). These regions are therefore poorly represented. The presence of a very large pool of dissolved organic matter in the SPG (Raimbault et al., 2008) can furthermore skew the results and lead to overestimation of remote primary production measurements (Claustre and Maritorena, 2003). Additionally, Dandonneau et al. (2003) argue, that floating particles can cause significant artifacts in chlorophyll sensing in oligotrophic waters, again leading to overestimations of J_{POC_A} .

3169

3.2 Coupling sediment-water interface and subsurface respiration

The low sedimentation rates in the SPG prevents labile organic carbon compounds from reaching deeper sediment layers and thus respiratory activity strongly drops with depth, as can be seen from the microprofiles (Fig. 4). The measured O_2 fluxes at the sediment-water interface are not exceptionally low. Nevertheless, because of the inert nature of the deeper sediment, any oxygen that escapes consumption in the surface layers is free to diffuse downwards and oxygenate deep layers. All piston cores within the central gyre were oxygenated for their entire length (up to 8 m, Fig. 1). The only station where oxygen did not penetrate to the base of the core is Station 12, farthest away from the center of the gyre, where oxygen penetrated about 1 m into the sediment. Generally, we observed a drop in oxygen concentration within the first meter from bottom water concentration to 170–180 $\mu\text{mol L}^{-1}$. All microsensor profiles, both, ex situ and in situ, showed a initial drop in concentration comparable to the decrease in the the deep profiles, but within the first few centimeters (Figs. 1 and 4). The slightly greater interval over which this decrease occurred in the piston cores most likely resulted from the piston coring process, mixing the top section of the cores (Buckley et al., 1994; Skinner and McCave, 2003).

The complete oxygenation of the sediment column in the SPG virtually excludes all other electron acceptors from use and the low overall respiration rates deep in the sediment effectively stretch the zone over which the aerobic degradation of organic matter occurs to several meters. Fitting exponential profiles through the data points below 1 m allowed for a robust extrapolation of the profiles down to the basalt, suggesting for the first time the presence of oxygen within the entire sediment column (Fig. 3). Respiration rates in the deeper layer appeared to be relatively constant with depth, a small flux between 0.04 and 0.5 $\mu\text{mol m}^{-2} \text{d}^{-1}$ was present.

The whole oxygen profile, including surface and deeper layers was modeled exemplary for Station 10, assuming exponentially decreasing respiration rates with depth, reflecting the dynamics in the first ~3–5 cm plus a constant term accounting for the

3170

deep respiration (Fig. 5). The exponential term can be explained by a pool of organic matter which is being exploited by the microbial community within the first centimeters of the sediment. Different interpretations are imaginable for the constant term: The deep respiration can be fueled by slow degradation of highly refractory, up to millions of years old organic matter. The exiguous decline of total organic carbon with depth in the deeper layers as reported by D'Hondt et al. (2009) would agree well with this. In this case, the low respiration term would not be constant but declining with such a low decrease with depth that it is not significantly different from a constant term.

Another explanation for the relatively constant deep respiration would be the radiolysis of water due to radioactive decays in sediment grains (D'Hondt et al., 2009; Blair et al., 2007; Jorgensen and D'Hondt, 2006; Lin et al., 2005). This process would split water in hydrogen and hydroxyl radicals. The hydrogen could act as electron donor while the hydroxyl radicals could further react to molecular oxygen. If this reaction is stoichiometric, the whole process is completely cryptic and is not reflected in the oxygen profiles at all, since the produced hydrogen and oxygen could be recombined microbially to water. If the hydroxyl radical, however, does not completely form molecular oxygen but further reacts with organic material or mineral surfaces, the additionally stimulated respiration could account for the constant respiration rate over depth that we observed.

The bioavailability of refractory organic matter can be enhanced by reaction with the highly reactive hydroxyl radicals formed by radiolysis, stimulating deep respiration. A similar process is well known for the degradation of organic matter with ultraviolet light (Benner and Biddanda; Moran and Zepp, 1997; Zafiriou, 2002).

3.3 Basement fluxes

To explore the possibility and consequences of oxygen fluxes from the sediment column to the basalt, a mathematical model of the reaction-diffusion process was set up and a parameter variation of flux and deep respiration was carried out (Eqs. 2 and 3). This model assumes steady state and constant respiration rates over depth as well

3171

as a constant flux into the basalt. Our model results indicate that there are several combinations of flux and respiration rate for each sampling site, for which the model gives satisfactory fits with the measured data. All of these parameter constellations fell along straight lines in the flux-respiration parameter space (Fig. 6). The higher the assumed respiration rate, the lower the flux into the basement. Very high respiration rates can only be explained if a net efflux of oxygen from the basalt to the sediment was assumed. The lines of best fit in the parameter space from the different sampling sites do not intercept the zero flux line at the same position (Fig. 7). Hence, if there is no flux to the basement at any station, very different respiration rates must occur at the different sites. On the other hand, if the respiration rate is the same at all of the sites, there must be different fluxes to the basement. The regions of best fit in the flux-respiration parameter space intercept in a small area of respiration rates below $\sim 6 \mu\text{mol m}^{-3} \text{yr}^{-1}$ and fluxes to the basalt in the range of -25 to $130 \mu\text{mol m}^{-2} \text{yr}^{-1}$. The sediments from Stations 1–11 are geochemically similar and microbial cell numbers are comparable for these many sites. Furthermore, high volumetric respiration rates are not supported by nitrate and alkalinity data (D'Hondt et al., 2009). Thus, a variable net flux of oxygen through the sediment into the basement at each site constitutes the most likely scenario, and leads to the question of possible sinks within the basalt. Oxygen could either be transported away by fluid flow within cracks and voids in the basalt (Fisher, 1998) or it could be reduced. One possibility would be the existence of a chemolithotrophic community within the basalt (Edwards et al., 2005; Stevens, 1997). Such communities were previously described for the flanks of the mid-ocean ridges (Ehrhardt et al., 2007; Huber et al., 2006) but their existence under the ocean basins remains controversial (Cowen et al., 2003). Drilling into the basalt under the SPG is necessary to further address this issue.

3.4 Regional and global relevance

Since we covered a large part of the SPG with our samples, we conclude that the total area of completely oxygenated sediments in this region is at least 10–15 million km^2 ,

3172

thus accounting for 3–4% of the global marine sediments. Murray and Grundmanis (1980) found oxygen to below 50 cm in equatorial Pacific sediments. Their oxygen profiles did not reach zero values but showed rather constant concentrations below an initial drop in the first several centimeters. Taking these findings into account, the oxygenated area is likely to be much larger, extending the deeply oxygenated sediment further north. Since the vast majority of all oxygen profiling measurements so far has been done in highly productive coastal areas or at ocean ridges (Seiter et al., 2005; Wenzhöfer and Glud, 2002), it is not unlikely that deep oxygen penetration also occurs in other low-productivity regions on earth, e.g. the North Pacific. Wenzhöfer et al. (2001) measured an in situ oxygen penetration depth of ~25 cm in the Atlantic; comparable ex situ oxygen penetration depths were measured by Loeff et al. (1990). Estimated carbon mineralization rates from the subtropical Atlantic gyre are in the order of 1.5–2 gC m⁻² yr⁻¹ (Wenzhöfer and Glud, 2002). These values are higher by a factor of 2 compared to the SPG. However, they are based only on few in situ measurements. Considering only the central sites (Station 6 and 7) this difference is even higher (factor 4), highlighting the extreme setting of the central SPG as the ultimate oceanic desert.

4 Conclusions

The aim of this work was to measure and analyze oxygen fluxes and respiration rates in sediments of the South Pacific Gyre, the most oligotrophic oceanic region on earth, and to obtain information about the magnitude and spatial organization of carbon turnover. While the benthic flux to the sediment is not extraordinary low compared to other oligotrophic sites, we found strong indications for oxygen penetrating down to the basalt in nearly the whole region. Respiration rates decrease strongly within the first few centimeters of the sediment and oxygen that is not reduced within this upper sediment horizon is free to diffuse further downwards. Even in the deeper layers, there is still a small and constant flux of oxygen.

3173

Acknowledgements. The authors would like to thank all participants of the KNOX-02RR cruise and the crew of the R/V Roger Revelle for their expert work. We particularly thank Franciszek Hasiuk and Andrea Stancin for the shipboard resistivity measurements used to calculate formation factor. Axel Nordhausen's technical assistance on board was most helpful. Without the work of Ingrid Dohrmann, Gabriele Eickert, Paul Färber, Volker Meyer, Ines Schröder and Cäcilia Wiegand this study would not have been possible. We thank the Integrated Ocean Drilling Program of the US National Science Foundation for funding the expedition. We also thank the Max Planck Society and the German National Science Program (DFG) IODP program for funding the lead author's participation in the expedition and for sponsoring our post-cruise research.

The service charges for this open access publication have been covered by the Max Planck Society.

References

- Antia, A., Koeve, W., Fischer, G., Blanz, T., Schulz-Bull, D., Scholten, J., Neuer, S., Kremling, K., Kuss, J., and Peinert, R.: Basin-wide particulate carbon flux in the Atlantic Ocean: Regional export patterns and potential for atmospheric CO₂ sequestration, *Global Biogeochem. Cycles*, 15, 845–862, 2001. 3167, 3169
- Archer, D., Emerson, S., and Smith, C.: Direct measurement of the diffusive sublayer at the deep sea floor using oxygen microelectrodes, *Nature*, 340, 623–626, 1989. 3163
- Barnett, P., Watson, J., and Connely, D.: A multiple corer for taking virtually undisturbed samples from shelf, bathyal and abyssal sediments, *Oceanologica Acta*, 7, 399–408, 1984. 3163
- Barrer, R.: Measurement of diffusion and thermal conductivity "constants" in non-homogeneous media, and in media where these "constants" depend respectively on concentration or temperature, *Proc. Phys. Soc.*, 58, 321–331, 1946. 3169
- Behrenfeld, M. and Falkowski, P.: A consumer's guide to phytoplankton primary productivity models, *Limnol. Oceanogr.*, 42, 1479–1491, 1997. 3167, 3169
- Bender, M. L. and Heggie, D. T.: Fate of organic carbon reaching the deep sea floor: a status report, *Geochim. Cosmochim. Acta*, 48, 977–986, 1984. 3160
- Benner, R. and Biddanda, B.: Photochemical Transformations of Surface and Deep Marine

3174

- Dissolved Organic Matter: Effects on Bacterial Growth, *Limnol. Oceanogr.*, 43, 1373–1378. 3171
- Berg, P., Rysgaard, S., Funch, P., and Sejr, M.: Effects of bioturbation on solutes and solids in marine sediments, *Aquat. Microb. Ecol.*, 26, 81–94, 2001. 3167
- 5 Berger, W. H., Fischer, K., Lai, C., and Wu, G.: Ocean productivity and organic carbon flux. I. Overview and Maps of Primary Production and Export Production., University of California, San Diego, SIO Reference, 87–30, 67 pp., 1987. 3167
- Berner, R.: *Early Diagenesis: A Theoretical Approach*, Princeton University Press, 1st edn., 1980. 3163, 3165
- 10 Betzer, P., Showers, W., Laws, E., Winn, C., Ditullio, G., and Kroopnick, P.: Primary productivity and particle fluxes on a transect of the equator at 153° W in the Pacific Ocean, *Deep-Sea Res. A*, 31, 1–11, 1984. 3167
- Blair, C. C., D'Hondt, S., Spivack, A. J., and Kingsley, R. H.: Radiolytic hydrogen and microbial respiration in subsurface sediments, *Astrobiology*, 7, 951–970, 2007. 3171
- 15 Buckley, D. E., MacKinnon, W. G., Cranston, R. E., and Christian, H. A.: Problems with piston core sampling: Mechanical and geochemical diagnosis, *Mar. Geol.*, 117, 95–106, 1994. 3165, 3170
- Claustre, H. and Maritorena, S.: The Many Shades of Ocean Blue, *Science*, 302, 1514–1515, 2003. 3161, 3169
- 20 Claustre, H., Huot, Y., Obernosterer, I., Gentili, B., Tailliez, D., and Lewis, M.: Gross community production and metabolic balance in the South Pacific Gyre, using a non intrusive bio-optical method, *Biogeosciences*, 5, 463–474, 2008, <http://www.biogeosciences.net/5/463/2008/>. 3161
- Cowen, J. P., Giovannoni, S. J., Kenig, F., Johnson, H. P., Butterfield, D., Rappe, M. S., Hutnak, M., and Lam, P.: Fluids from Aging Ocean Crust That Support Microbial Life, *Science*, 299, 120–123, 2003. 3172
- 25 Dandonneau, Y., Vega, A., Loisel, H., du Penhoat, Y., and Menkes, C.: Oceanic Rossby Waves Acting As a “Hay Rake” for Ecosystem Floating By-Products, *Science*, 302, 1548–1551, 2003. 3169
- 30 Daneri, G. and Quinones, R.: Undersampled Ocean systems: a plea for an international study of biogeochemical cycles in the Southern Pacific Gyre and its boundaries, *US JGOFS Newsletter* January, 9, 2001. 3161
- D'Hondt, S., Spivack, A. J., Pockalny, R., Fischer, J. P., Kallmeyer, J., Ferdelman, T., Abrams,

3175

- L., Smith, D. C., Graham, D., Hasiuk, F., Schrumm, H., and Stancin, A. M.: Subseafloor Sedimentary Life in the South Pacific Gyre, *Proc. Nat. Acad. Sci. USA*, in review, 2009. 3161, 3171, 3172, 3179
- 5 Edwards, K. J., Bach, W., and McCollom, T. M.: Geomicrobiology in oceanography: microbe-mineral interactions at and below the seafloor, *Trends in Microbiology*, 13, 449–456, 2005. 3172
- Ehrhardt, C. J., Haymon, R. M., Lamontagne, M. G., and Holden, P. A.: Evidence for hydrothermal Archaea within the basaltic flanks of the East Pacific Rise, *Environ. Microbio.*, 9, 900–912, 2007. 3172
- 10 Fisher, A.: Permeability within basaltic oceanic crust, *Rev. Geophys.*, 36, 143–182, 1998. 3172
- Glud, R., Gundersen, J., Jørgensen, B., Revsbech, N., and Schulz, H.: Diffusive and total oxygen uptake of deep-sea sediments in the eastern South Atlantic Ocean: in situ and laboratory measurements, *Deep Sea Res.*, 41, 1767–1788, 1994. 3163, 3168
- 15 Huber, J. A., Johnson, H. P., Butterfield, D. A., and Baross, J. A.: Microbial life in ridge flank crustal fluids, *Environ. Microbio.*, 8, 88–99, 2006. 3172
- Jahnke, R.: The global ocean flux of particulate organic carbon: Areal distribution and magnitude, *Global Biogeochem. Cycles*, 10, 71–88, 1996. 3168, 3169
- Jørgensen, B. B. and D'Hondt, S.: A Starving Majority Deep Beneath the Seafloor, *Science*, 314, 932–934, 2006. 3171
- 20 Klimant, I., Meyer, V., and Kühl, M.: Fiber-optic oxygen microsensors, a new tool in aquatic biology, *Limnol. Oceanogr.*, 40, 1159–1165, 1995. 3164
- Li, Y.-H. and Gregory, S.: Diffusion of ions in sea water and in deep-sea sediments, *Geochim. Cosmochim. Acta*, 38, 703–714, 1974. 3166
- 25 Lin, L., Hall, J., Lippmann-Pipke, J., Ward, J., Lollar, B., DeFlaun, M., Rothmel, R., Moser, D., Gihring, T., Mislowack, B., et al.: Radiolytic H₂ in the continental crust: nuclear power for deep subsurface microbial communities, *Geochem. Geophys. Geosyst.*, 6, Q07003, doi:10.1029/2004GC000907, 2005. 3171
- Loeff, M., Meadows, P., and Allen, J.: Oxygen in Pore Waters of Deep-Sea Sediments [and Discussion], *Philos. Trans. R. Soc. London, Ser. A*, 331, 69–84, 1990. 3173
- 30 Moran, M. A. and Zepp, R. G.: Role of Photoreactions in the Formation of Biologically Labile Compounds from Dissolved Organic Matter, *Limnol. Oceanogr.*, 42, 1307–1316, 1997. 3171
- Morel, A., Gentili, B., Claustre, H., Babin, M., Bricaud, A., Ras, J., and Tiche, F.: Optical properties of the “clearest” natural waters, *Limnol. Oceanogr.*, 52, 217–229, 2007. 3161

3176

- Murray, J. and Kuivila, K.: Organic matter diagenesis in the northeast Pacific: transition from aerobic red clay to suboxic hemipelagic sediments, *Deep-Sea Res. I*, 37, 59–80, 1990. 3169
- Murray, J. W. and Grundmanis, V.: Oxygen Consumption in Pelagic Marine Sediments, *Science*, 209, 1527–1530, 1980. 3161, 3168, 3173
- 5 Pace, M. L., Knauer, G. A., Karl, D. M., and Martin, J. H.: Primary production, new production and vertical flux in the eastern Pacific Ocean, *Science*, 235, 803–804, 1987. 3167
- Raimbault, P., Garcia, N., and Cerutti, F.: Distribution of inorganic and organic nutrients in the South Pacific Ocean – evidence for long-term accumulation of organic matter in nitrogen-depleted waters, *Biogeosciences*, 5, 281–298, 2008,
 10 <http://www.biogeosciences.net/5/281/2008/>. 3169
- Ras, J., Claustre, H., and Uitz, J.: Spatial variability of phytoplankton pigment distributions in the Subtropical South Pacific Ocean: comparison between in situ and predicted data, *Biogeosciences*, 5, 353–369, 2008,
 15 <http://www.biogeosciences.net/5/353/2008/>. 3161
- Rasmussen, H. J. B. B.: Microelectrode studies of seasonal oxygen uptake in a coastal sediment: Role of molecular diffusion., *Mar. Ecol. Prog. Ser.*, 81, 289–303, 1992. 3163
- Reimers, C. E., Fischer, K. M., Merewether, R., Smith, K. L., and Jahnke, R. A.: Oxygen microprofiles measured in situ in deep ocean sediments, *Nature*, 320, 741–744, 1986. 3162
- Revsbech, N.: An Oxygen Microsensor with a Guard Cathode, *Limnol. Oceanogr.*, 34, 474–
 20 478, 1989. 3163
- Revsbech, N. and Jørgensen, B.: Photosynthesis of benthic microflora measured with high spatial resolution by the oxygen microprofile method: capabilities and limitations of the method, *Limnol. Oceanogr.*, 28, 749–756, 1983. 3163
- Schulz, H. and Zabel, M.: *Marine Geochemistry*, Springer, 2000. 3165
- 25 Seiter, K., Hensen, C., and Zabel, M.: Benthic carbon mineralization on a global scale, *Global Biogeochem. Cycles*, 19, GB1010, doi:10.1029/2004GB002225, 2005. 3173
- Skinner, L. C. and McCave, I. N.: Analysis and modelling of gravity- and piston coring based on soil mechanics, *Marine Geology*, 199, 181–204, 2003. 3165, 3170
- Stevens, T.: Lithoautotrophy in the subsurface, *FEMS Microbiol. Rev.*, 20, 327–337, 1997. 3172
- 30 Suess, E.: Particulate organic carbon flux in the oceans – surface productivity and oxygen utilization, *Nature*, 288, 260–263, 1980. 3167
- Thamdrup, B. and Canfield, D. E. (Eds.): *Benthic Respiration in Aquatic Sediments*, *Methods in Ecosystem Science*, Springer-Verlag, New York, 1th edn., 2000. 3160

3177

- Wenzhöfer, F. and Glud, R.: Benthic carbon mineralization in the Atlantic: a synthesis based on in situ data from the last decade, *Deep-Sea Res. I*, 49, 1255–1279, 2002. 3162, 3163, 3168, 3173
- Wenzhöfer, F., Holby, O., and Kohls, O.: Deep penetrating benthic oxygen profiles measured in
 5 situ by oxygen optodes, *Deep-Sea Res. I*, 48, 1741–1755, 2001. 3161, 3164, 3168, 3173
- Zafiriou, O.: Sunburnt organic matter: biogeochemistry of light-altered substrates, *Limnol. Oceanogr. Bull.*, 11, 69–74, 2002. 3171

3178

Table 1. Sampling positions, waterdepth [m], sediment thickness [m], diffusive oxygen uptake (DOU) and fluxes of particulate organic matter as calculated from primary production (J_{POC_A}) or using the oxygen fluxes (J_{POC_R}). Units: DOU: $\text{mmol m}^{-2} \text{d}^{-1}$; PP , J_{POC_A} , J_{POC_R} : $\text{gC m}^{-2} \text{yr}^{-1}$. Sediment thicknesses after D'Hondt et al. (2009).

| Stat. | Lat | Lon | W. depth | Sed. thick | DOU | J_{POC_R} | PP | J_{POC_A} |
|-------|----------|-----------|----------|------------|-------|-------------|------|-------------|
| 1 | -32° 51' | -165° 39' | 5697 | 71 | – | – | 77 | 0.61 |
| 2 | -26° 03' | -156° 54' | 5127 | 17 | – | – | 83 | 0.75 |
| 3 | -27° 57' | -148° 35' | 4852 | 5.5 | – | – | 86 | 0.83 |
| 4 | -26° 29' | -137° 56' | 4285 | 9.4 | -0.27 | 0.89 | 72 | 0.66 |
| 5 | -28° 27' | -131° 23' | 4221 | 16.5 | -0.20 | 0.66 | 77 | 0.75 |
| 6 | -27° 55' | -123° 10' | 3738 | 15 | -0.15 | 0.52 | 70 | 0.69 |
| 7 | -27° 44' | -117° 37' | 3170 | 1.5 | -0.13 | 0.45 | 66 | 0.69 |
| 9 | -38° 03' | -133° 05' | 3250 | 19.8 | – | – | 118 | 1.90 |
| 10 | -39° 19' | -139° 48' | 3760 | 21.4 | -0.32 | 1.06 | 113 | 1.60 |
| 11 | -41° 51' | -153° 06' | 4190 | 67 | – | – | 130 | 1.90 |
| 12 | -45° 58' | -163° 11' | 4600 | 130 | – | – | 157 | 2.49 |

3179

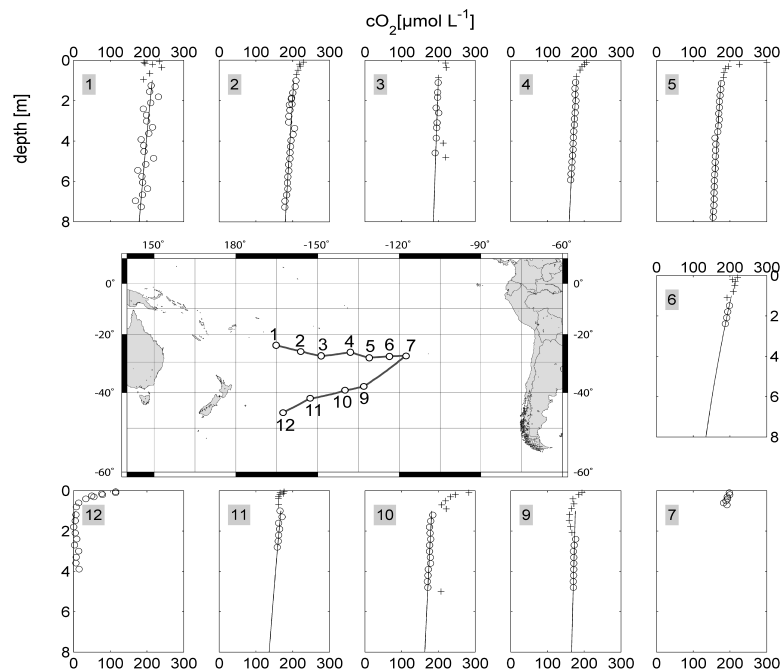


Fig. 1. Sampling stations in the South Pacific (middle) and deep oxygen profiles at the respective positions. The solid line represents exponential extrapolations of the deep data points (open symbols). Crosses: Data points not used for extrapolation.

3180

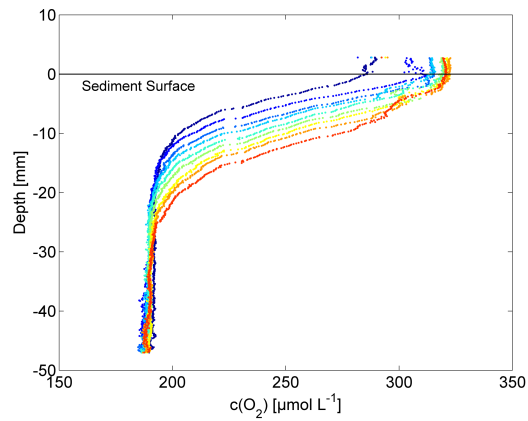


Fig. 2. Transient microsensor profiles measured ex-situ on a multi-core. The oxygen concentration in the overlaying water was changed from $280 \mu\text{mol L}^{-1}$ to $320 \mu\text{mol L}^{-1}$. The time between subsequent profiles was two hours.

3181

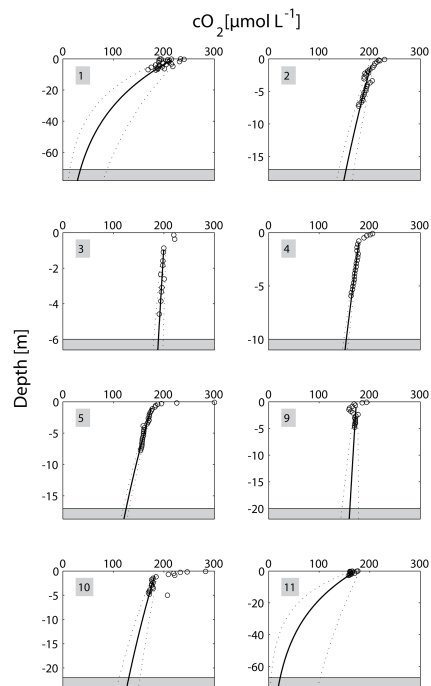


Fig. 3. Extrapolated profiles of oxygen concentration of 8 different stations down to the basalt (grey bar). Circles indicate measured oxygen concentrations, solid lines depict the exponential model and dotted lines show the 90% confidence bounds for the fit.

3182

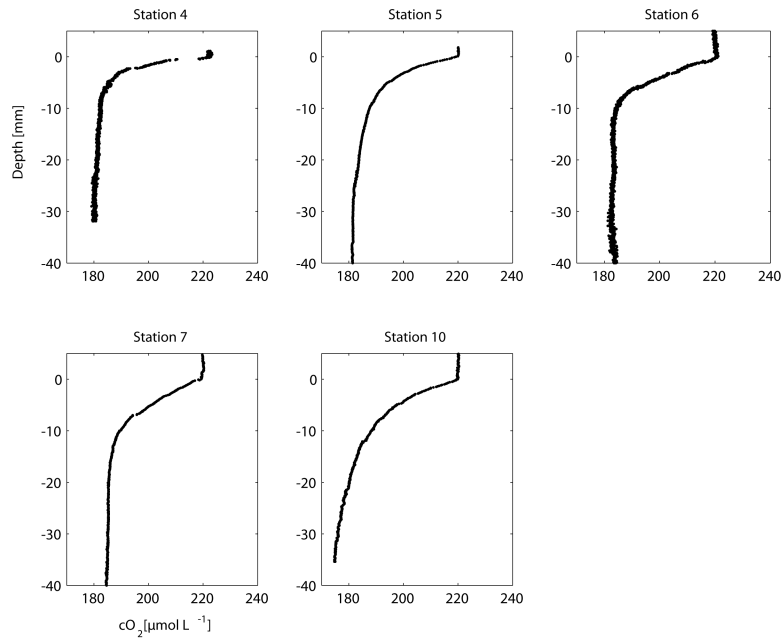


Fig. 4. Microsensor profiles measured ex-situ (Station 4–7) and in-situ (Station 10).

3183

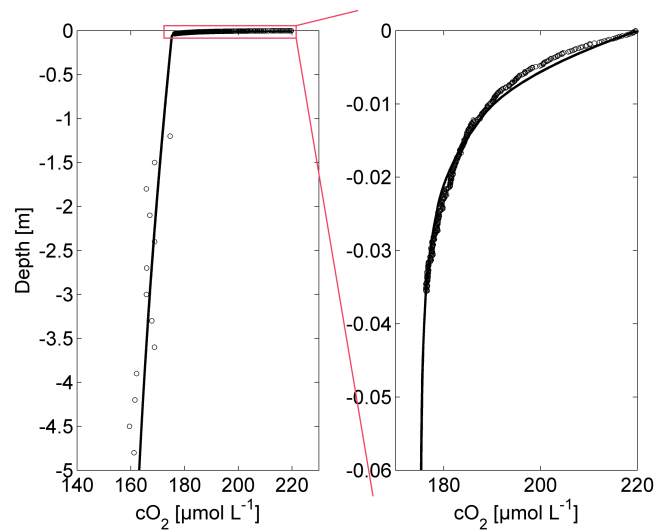


Fig. 5. Left: composed profile of Station 10, using data from piston core measurements and in-situ profiling (open symbols) and fitted model with exponentially decreasing respiration rates with constant offset (solid line). Right: magnification of the top 6 cm of the profile, showing the microsensor data and the model.

3184

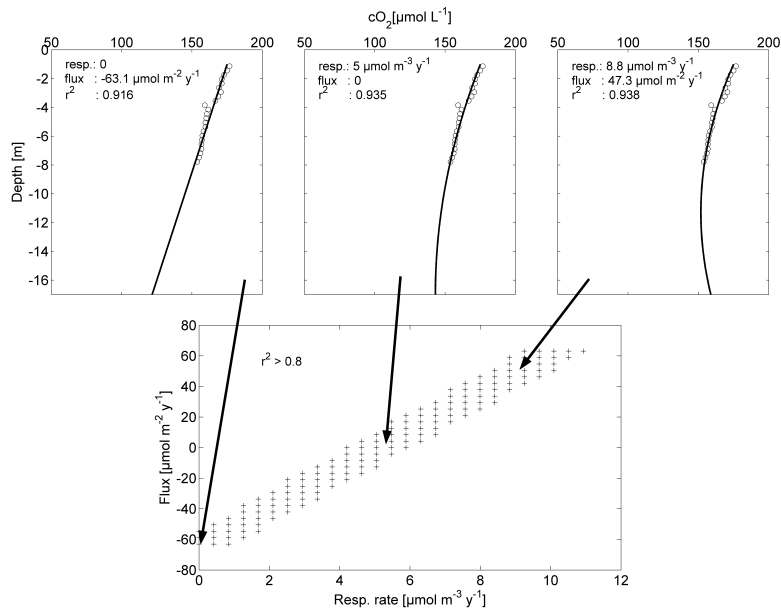


Fig. 6. Top: three scenarios of different respiration rates and fluxes to the basalt (lines), which provide good fits to the measured data of Station 10 (open symbols). Bottom: area in the parameter space, which provides good fits ($r^2 > 0.8$) to the data.

3185

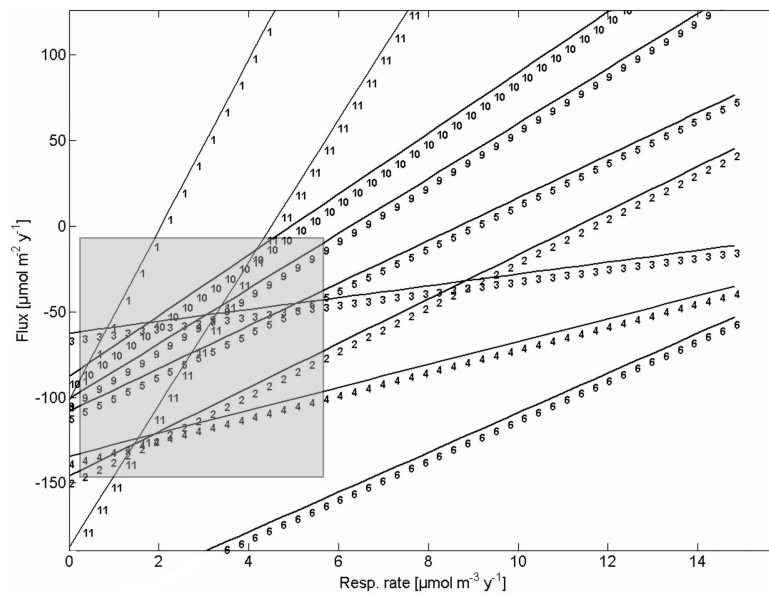


Fig. 7. Lines of best fits in the respiration/flux parameter space, as determined by parameter variation of a model for the deep oxygen profiles. The shaded area depicts the most plausible parameter combinations (see text). Negative values: flux sediment→basalt.

3186